RSC Advances

ROYAL SOCIETY OF CHEMISTRY

www.rsc.org/advances

Table of contents entry

$CuInS_2$ absorber films were manufactured via sulfurization of Cu-In precursors that were electrodeposited from a simple acidic solution without any complexing agent.

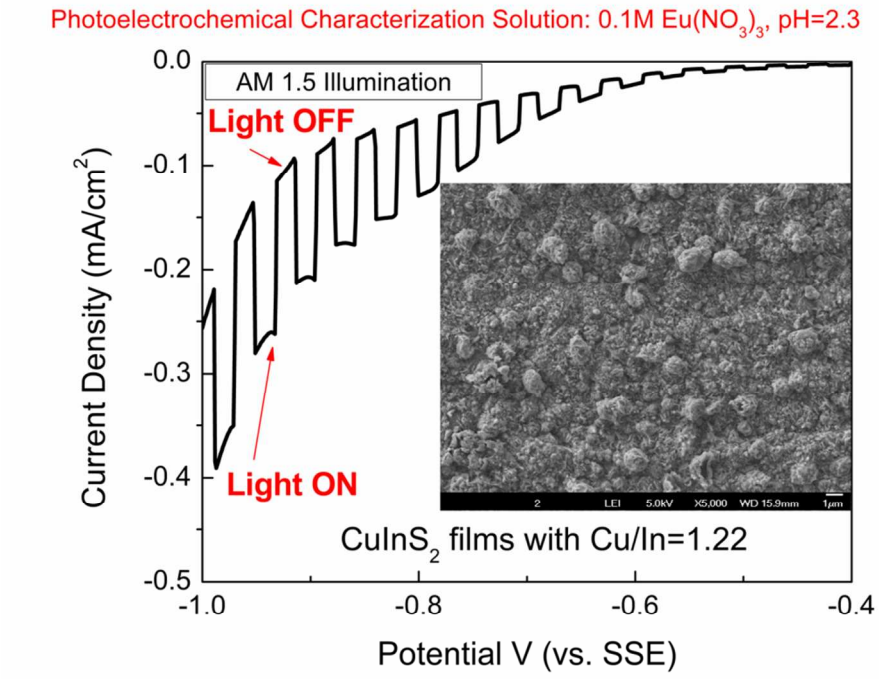

Formation of p-type $CuInS_2$ absorber layers via sulfurization of co-electrodeposited Cu-In precursors

Begum Unveroglu and Giovanni Zangari

Department of Materials Science and Engineering and CESE,
University of Virginia, Charlottesville 22904 VA, USA

Abstract

The electrodeposition of Cu-In alloy precursors with suitable stoichiometry and consisting mainly of intermetallic compounds, followed by sulfurization, is a promising method to form good quality $CuInS_2$ thin films. In this work, Cu-In precursors forming intermetallic compounds were electrodeposited from an acidic solution on Mo substrates at 50°C and sulfurized to form p-type $CuInS_2$ absorber layers. We studied the crystal structure and compositional characteristics of films before and after sulfurization. Intermetallic compounds, namely $Cu_{11}In_9$ and Cu_9In_4, have been observed for precursor films suitable to form $CuInS_2$, and p-type $CuInS_2$ phase with small amounts of CuS was formed, showing the chalcopyrite and CuAu-type ordered phases for Cu/In ratios between 1.09-1.34. The carrier density was increased with increasing Cu/In ratio, but the photoelectrochemical response of the films was not directly related to this ratio. Film morphology has a critical influence on the photocurrent response. The highest photoelectrochemical current was achieved from compact and smooth precursors that were electrodeposited at -1.3V while the lowest value was obtained with a rough dendritic precursor that was electrodeposited at -1.6V.

Keywords: Co-electrodeposition, $CuInS_2$, $Cu_{11}In_9$, photovoltaics, photoelectrochemical characterization

Introduction

The increased global demand for renewable, CO_2 neutral energy sources underscores the need for the development of existing renewable energy technologies to the point where worldwide deployment may become feasible and commercially viable. Solar photovoltaic (PV) technology is a promising green energy source whose output has increased steadily over time, reaching in 2012 a global operating capacity of 100 GW [1]. While crystalline silicon dominates the market, amorphous silicon and thin film technologies such as cadmium telluride and copper indium gallium selenide/sulfide have grown steadily [2–5]. Among these, the production of silicon-based solar cells is costly, due to the amount and the price of material being used, while cadmium telluride thin film solar cells contain toxic elements, hindering success in the PV market [6]. Alternative low cost and less toxic solar cells are chalcopyrite based thin films; these are suitable for optoelectronic devices due to their direct bandgap and high absorption coefficient [7,8]. The $CuInGaSe_2$ absorber layer based solar cells have reached up to 20% efficiency,however, the high cost of Ga and the toxic character of Se are still plaguing the widespread development of these PV cells [5]. $CuInS_2$ films, on the other hand, are promising candidates for PV absorber layers, due to the overall lower material cost and fewer toxic compounds in comparison with $CuInGaSe_2$ absorber layers [9]. The theoretical efficiency for homo-junction thin film devices is close to 23 % and the simulated efficiency of a $CuInS_2$ solar cell with a traditional structure, Al/ZnO: Al/n-CdS/p-$CuInS_2$/Mo with optimum thickness can reach up to 20.4% [10,11]. However, the laboratory efficiencies of $CuInS_2$ based solar cells are still only around 11-12% [12,13]. Further studies on the influence of composition, crystal structure, and growth mechanisms aiming at improved phase purity are needed to approach the predicted laboratory efficiency.

Manufacturing methods for $CuInS_2$ include vacuum techniques such as molecular beam epitaxy, reactive magnetron sputtering, and chemical vapor deposition, as well as non-vacuum techniques such as chemical bath deposition, spray pyrolysis, sol-gel, and electrochemical deposition [14-22]. In particular, the latter provides simple, inexpensive and scalable production of large area films coupled with close control over the growth process [23]. Electrodeposition may produce $CuInS_2$ films through one of three methods: (i) simultaneous deposition of all the elements, (ii) sequential deposition of the metallic element followed by sulfurization, and (iii) electrodeposition of Cu-In alloy precursors followed by sulfurization [20-25]. Electrodeposition of Cu-In alloys has been shown to yield intermetallic

compounds in the as-deposited films [12,26, 27]**;** this is advantageous since $Cu_{11}In_9$ has been reported to be a most suitable precursor for $CuInS_2$ formation [26]. Kind et al. for example prepared citrate-capped $Cu_{11}In_9$ nanoparticles to form $CuInS_2$, and the resulting material efficiency reached up to 7% [28]. One of the record efficiency, 11%, for Cu-rich $CuInS_2$ was obtained by pre-annealing the Cu/In layers at 155°C to form $Cu_{11}In_9$ before the sulfurization process [12].

This work is concerned with the synthesis of $CuInS_2$ absorber layers via electrodeposition of an alloy precursor followed by sulfurization from the gas phase. In this process, a uniform composition of the precursor material is paramount, due to its influence on the defect chemistry, the band gap and the efficiency of the final CIS material [29,30]. In particular, it has been reported that Cu-rich precursors exhibit better efficiencies than Cu-poor precursor films [12, 13,31-33]. In the early 1990s, a 10.2% efficiency was obtained from a Cu-rich precursor that forms close to stoichiometric $CuInS_2$ (Cu/In film ratio 0.98); later, Na-incorporated Cu-poor precursors with Cu/In precursor ratio 0.90 reached up to 10.6% efficiency [32,33]. The highest recorded efficiency is so far 12.5%, achieved in $CuInS_2$ film obtained from Cu-rich precursor, Cu/In ratio 1.8, which formed stoichiometric $CuInS_2$ film [13]. In their study, Klaer et al. showed that the efficiency increased with the increasing precursor Cu/In ratio for a compositional ratio between 1.0 and 1.8. Cu-rich precursors form sufficient amount of CuS which supports the growth of chalcopyrite and sulfur incorporation as reported in ref [13]. These reported efficiency values demonstrate the importance of the Cu-rich precursors to obtain high efficiencies in $CuInS_2$ films.

In general, besides the compositional ratio, minimization of the secondary phases and control over the different crystal structures of $CuInS_2$ are all crucial for the quality of absorber layers. Cu-poor films form $CuIn_5S_8$ and β-In_2S_3 while Cu-rich films forms CuS segregating at the surface [34]; the latter can be removed by etching with KCN. In addition, the formation of MoS_2 at the substrate/absorber interface is less pronounced for Cu-rich than Cu-poor films [35]. $CuInS_2$ exhibits three metastable semiconducting phases: a cubic CuPt-type ordered phase, hexagonal CuAu-type ordered phases and the tetragonal chalcopyrite phase [36,37]. The latter two phases can co-exist in the same material [38,39]. Lee et al. reported the presence of both phases after sulfurization of precursors with different Cu/In ratios [38]. In their work, sulfurized metallic precursors have been reported to exhibit better crystallinity

than $CuInS_2$ films obtained by spray pyrolysis [38]. This result suggests that the manufacturing method of $CuInS_2$ plays a critical role in the quality of the solar cell.

The aim of this study is to form Cu-In precursors with controlled and uniform film composition, in order to investigate the influence of precursor features such as crystal structure and morphology on the performance of the final absorber compound. Precursors are found to contain intermetallic compounds, predominantly $Cu_{11}In_9$, with a small amount of elemental indium. The resulting sulfurized Cu-In precursors formed Cu-rich and Cu-poor $CuInS_2$ films with a mixed phase of chalcopyrite and CuAu-type ordered phases. Significant photoelectrochemical response was observed for Cu-rich films with Cu/In ratio 1.09 -1.34. The highest photoelectrochemical current was detected for a compact and uniform film with a Cu/In ratio of 1.22 after sulfurization, which was electrodeposited at low overpotentials.

Experimental Details

Film growth was performed in a three-electrode electrochemical cell. A Pt mesh was used as a counter electrode, and a saturated mercurous sulfate reference electrode (SSE, $E^o_{SSE} = 0.650V_{SHE}$) was placed in a different compartment, separated from the main one by a capillary. The experiments were performed using an EG&G-PAR potentiostat-galvanostat Model 263A. Electrochemical co-deposition of the Cu-In precursors was performed at 50°C. The cell temperature was maintained by immersing the main compartment of the cell in a hot water jacket circulator (Neslab Ex7); the reference electrode was separated from the heated solution in order to operate at room temperature. The Cu-In films were grown from a 0.5M H_2SO_4 acidic solution containing 0.5-15mM $CuSO_4$ and 25mM $In_2(SO_4)_3$. The solutions were made using ultra-pure Milli-Q water (resistivity18.2 MΩ·cm) produced in house.

The working electrode substrate was a Mo sheet with 0.1mm thickness and 99.95% purity (Alfa Aesar). The size of the precursor films was ~ 1 cm^2. Before deposition, the Mo foils were first subjected to sequential cleaning in acetone, isopropanol, and ethanol (30' for each solution). Then, the Mo substrate was etched in 25 vol% NH_4OH solution for 3', rinsed and used immediately after that. The deposition time was varied between 9 and 30 minutes. The thickness of the films ranged between 3 and 7 μm.

The sulfurization of the Cu-In precursors was performed at 500°C for 1 hour in a sealed quartz tube using an Ar atmosphere. Sulfur pellets with 99.99% purity (Alfa Aesar) were used as the sulfur source. After annealing, the furnace was turned off, and films were

naturally cooled, while still in the tube, down to room temperature. No etching of secondary phases was performed.

A liquid junction cell was used to investigate the photoelectrochemical response of the films. A suitable redox couple for the $CuInS_2$ films is Eu^{2+}/Eu^{3+} [40,41]. Photoelectrochemical characterization of the films was performed in a custom made cell containing 0.1M $Eu(NO_3)_3$ (Alfa Aesar) solution using a standard three-electrode configuration. The pH of the solution was adjusted to 2.3 with dilute H_2SO_4. Mott-Schottky measurements were performed in 0.1M Na_2SO_4 solution at pH 5.8 and the frequency used for measurements was 10 kHz. The photoelectrochemical current spectra and Mott-Schottky data were recorded using an SP 150 BioLogic potentiostat. Photoelectrochemical characterizations were performed under simulated sunlight (Oriel Sol 1A, Newport).

The crystal structure of the films was determined by X-ray diffraction (XRD), using a PANalytical X'Pert Pro MPD instrument with Cu Kα radiation (λ = 1.5406 Å) in a Bragg-Brentano configuration. The surface morphology of Cu-In films before and after sulfurization was examined with an FEI Quanta 650 Scanning Electron Microscope (SEM). The film composition was measured with an energy dispersive X-ray spectrometry (EDX) detector attached to the SEM; the accelerating voltage was 20kV. Raman spectra of the $CuInS_2$ films were obtained using a Renishaw inVia Raman microscope with an excitation wavelength of 514 nm.

Results and discussion

Composition of the as-deposited precursors and annealed films

Cu-In alloy precursors with Cu between 7.3 and 89.5 at% have been electrochemically deposited from a simple acidic solution without any complexing agent. **Fig. 1.a** shows the copper atomic fraction of alloys deposited on molybdenum substrates as determined by EDX. The level of oxygen impurities is always less than 3 at% for the annealed films. Three different solutions were studied (solutions 1, 2 and 3), containing 0.5, 1.0 and 1.5 mM Cu^{2+}, respectively. The Cu fraction first decreased with decreasing applied potential, eventually reaching a plateau, possibly a consequence of growth under diffusion limiting conditions. The maximum indium fraction was observed around -1.3V for sol. 1 and -1.2V for solutions 2 and 3[**Fig. 1.a**]. Increasing [Cu^{2+}] in the solution increased the corresponding limiting current density and the Cu fraction in the films, thus decreasing the In fraction at the same deposition

potentials [**Fig. 1.a**]. Cu-rich precursors close to Cu/In ~ 1, suitable for the formation of $CuInS_2$ semiconductor films, were obtained with a high [Cu^{2+}], in sol. 3 at deposition potentials between -1.2 and -1.6V. The Cu/In ratios of precursor films, before and after sulfurization, are reported in **Fig. 1.b**; before sulfurization in the selected potential range this ratio is between 0.78 and 1.17. Due to indium evaporative loss during the heat treatment, the Cu/In ratio increased for all films after sulfurization [42], resulting in a Cu/In ratio between 0.86 and 1.34.These films are characterized and discussed in detail in the following section.

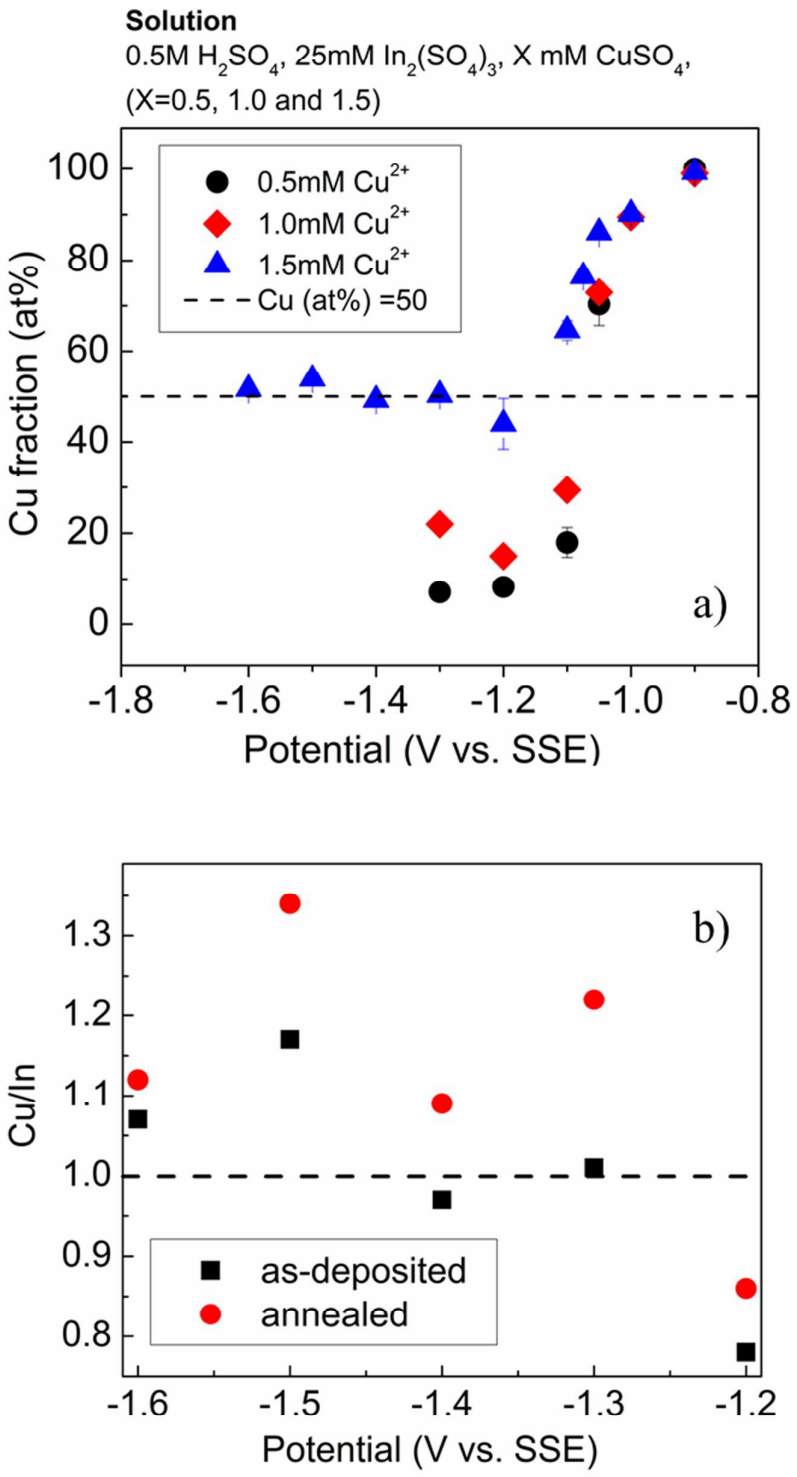

Fig. 1 a) Composition of the as-deposited precursor films and **b)** Cu/In ratio for precursors before and after sulfurization for precursor films electrodeposited from sol. 3.

Crystal structure of the as-deposited precursors and annealed films

The as-deposited films consist of elemental indium and intermetallic compounds, including $Cu_{11}In_9$ and Cu_9In_4, in a ratio dependent on the average composition. The concentration of copper ions in solution strongly affected codeposition conditions, hence the crystal structure of the precursor films; specifically, precursors deposited from solutions containing 0.5-1.0mM Cu^{2+} ions mainly contain elemental indium, with a low fraction of intermetallic compounds. The XRD patterns for films deposited from a solution with 1.5mM $CuSO_4$ and 25mM $In_2(SO_4)_3$ between the deposition potentials -1.1V and -1.6V are shown in **Fig. 2**; all these alloys exhibit reflections corresponding to intermetallic compounds (IMCs) and elemental indium. The fraction of the IMCs increases with higher overpotentials as a result of enhanced nucleation of these phases in correspondence of larger applied driving forces. $Cu_{11}In_9$ is the major compound for the given set of precursor films in **Fig. 2**.

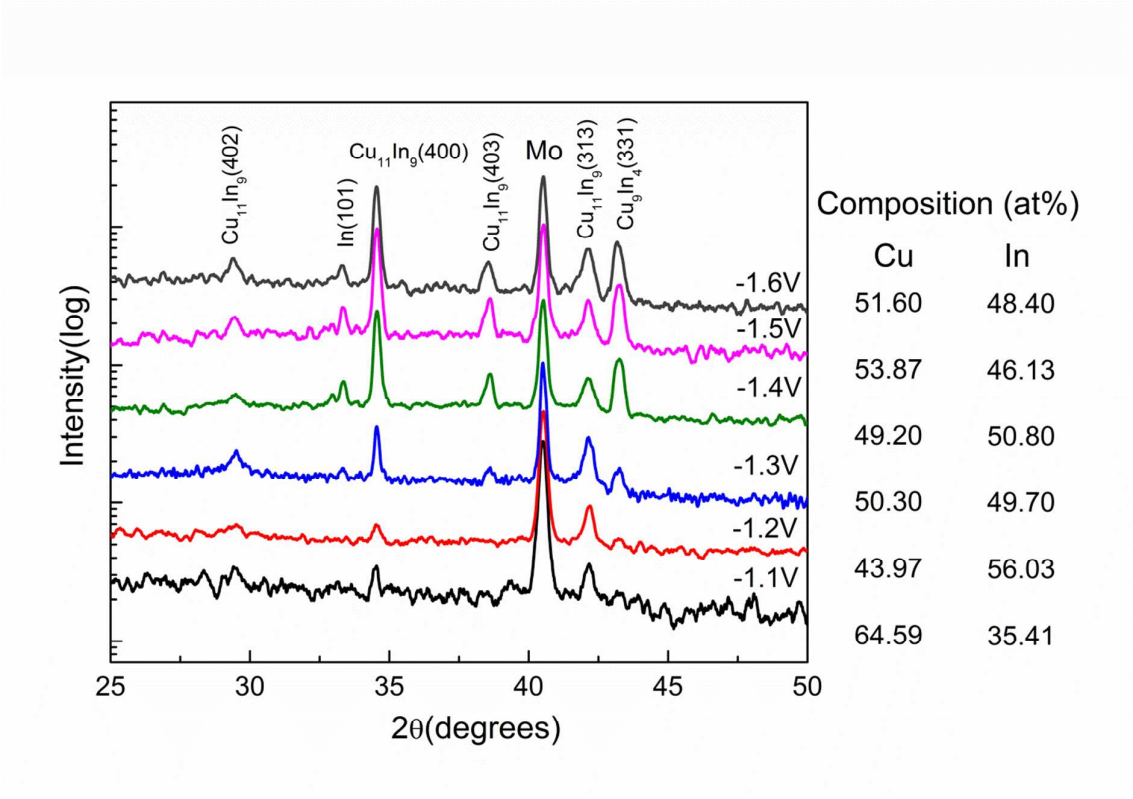

Fig. 2 XRD patterns of the Cu-In precursors electrodeposited from sol. 3, which contains 1.5 mM $CuSO_4$, 25mM $In_2(SO_4)_3$, 0.5M H_2SO_4.

After sulfurization, XRD patterns of most films grown from the first two solutions formed an In-rich $CuIn_5S_8$ phase, while only a few Cu-rich precursor films deposited at less negative potentials developed a $CuInS_2$ phase. Secondary phases in XRD patterns include Covellite and hexagonal CuS, commonly found in $CuInS_2$ films. XRD patterns of sulfurized films grown from the solution with 1.5 mM Cu^{2+} at -1.1V to -1.6V are shown in **Fig. 3**. The $CuInS_2$ phase was observed for all the films while CuS was detected for all films except those deposited at -1.3V. The latter consists predominantly of $Cu_{11}In_9$ and shows the minimum amount of elemental indium and Cu_9In_4. Klopmann et al. proposed that the formation of the $CuInS_2$ phase starts close to 255°C by consumption of $Cu_{11}In_9$ according to the reaction given below [43];

$$4Cu_{11}In_9 + 9S_8 \rightarrow 36CuInS_2 + 8Cu \quad (1)$$

It has been reported that Cu-poor films and the stoichiometric precursors form $CuIn_5S_8$ in addition to $CuInS_2$ [43]. However, in our study, the formation of $CuIn_5S_8$ has not been observed for close to stoichiometric or Cu-poor films. This may be due to different synthesis of the starting materials. In the study of Klopmann et al., $CuInS_2$ films were obtained via sulfurization of a bilayer structure, indium on top of a copper layer. In the present work instead, the formation of $CuInS_2$ is taking place via sulfurization of precursors which consist predominantly of $Cu_{11}In_9$ intermetallics and a small amount of elemental Indium.

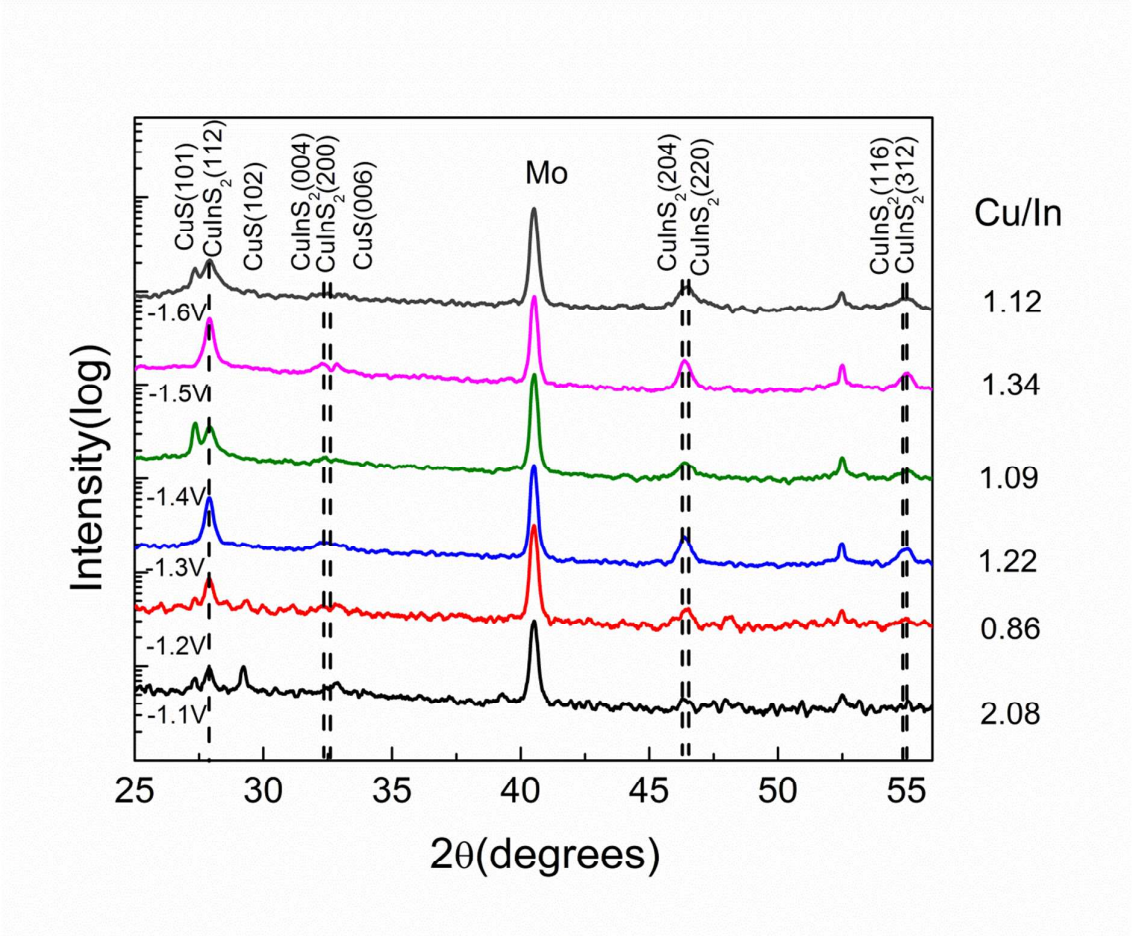

Fig. 3 XRD patterns of annealed Cu-In precursors electrodeposited from sol. 3, which contains 1.5 mM $CuSO_4$, 25mM $In_2(SO_4)_3$, 0.5M H_2SO_4.

Microstructure of the as-deposited precursors and annealed films

The microstructure of Cu-In alloy precursors deposited at potentials between -1.1V and -1.4V from sol. 3, and their sulfurized counterparts are shown in **Fig. 4**. The Cu/In ratio for each film is given in the figures. The morphology of Cu-In films changed from fine particulates with uniform size at -1.1 V to rough films with dendrites at the potential of -1.4 V [**Fig. 4.a-d**].

Diffusion limiting conditions strongly influence film morphology, favoring in the general formation of dendrites and porous structures. We calculated the diffusion limiting current for 1.5 mM copper (1.5mM $CuSO_4$) and 50 mM indium (25mM $In_2(SO_4)_3$) , assuming a Nernst diffusion layer thickness of 0.5 mm and diffusion coefficient for both Cu^{2+} and In^{3+} at 10^{-5} cm^2/s, independent of ion concentration and temperature. The estimated diffusion limiting

current for Cu is $5.79x10^{-2}$ mA/cm^2 and for In is 2.9mA/cm^2. The measured current density for precursor films deposited at potential -1.1V, 50ºC is slightly less than 2.9mA/cm^2. At more negative potentials -1.2 and -1.3V the current density increases to 9.5 and 35mA/cm^2, respectively. These values are above the calculated limiting current. However, compact and uniform film are still obtained under these conditions. In our previous study, the onset of hydrogen evolution HER in the Cu-In solution at 50°C on gold was observed at about -1.15V [27]. The HER is vigorous enough to enhance diffusion near the electrode layer, possibly increasing the limiting current above that under stagnant conditions, explaining the growth of compact films with relatively well-defined crystallites [44]. Much above the diffusion limiting current, at potential below -1.4V, films began to show dendritic growth as expected.

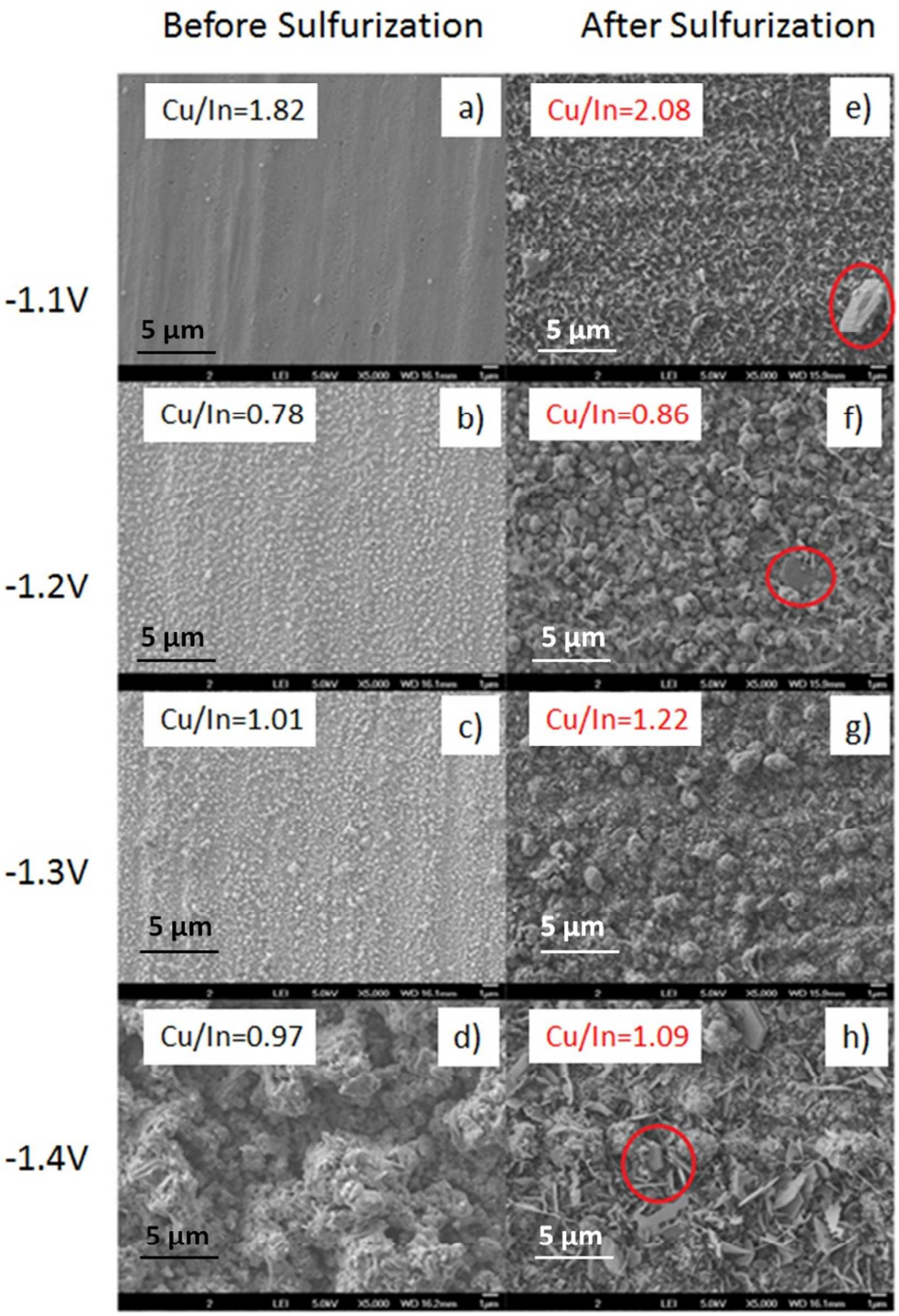

Fig. 4 Microstructure of electrodeposited Cu-In precursors at potentials a)-1.1, b)-1.2. c) -1.3 and d) -1.4V and after sulfurization, precursor deposition potentials e)-1.1, f)-1.2. g) -1.3 and h) -1.4V.

A CuS secondary phase is visible on the film surface after sulfurization in the form of hexagonal shaped particles as highlighted by circles in **Fig. 4e-h**. The cross sections of the films deposited at -1.3V and -1.6V before and after sulfurization are shown in **Fig. 5**. These images confirm the above observation that current densities slightly above the diffusion limiting current resulted in a smooth surface and compact as well as dense film, while more negative deposition potentials resulted in the formation of dendrites.

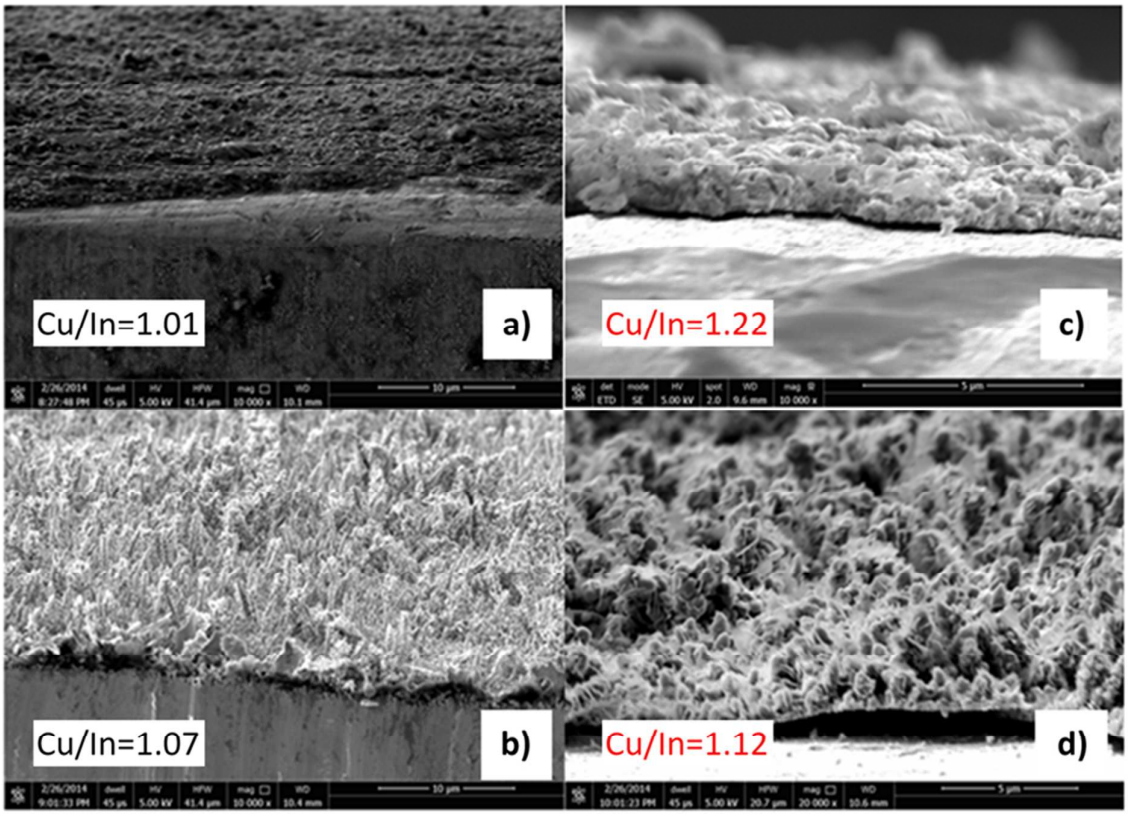

Fig. 5 Cross-section images of Cu-In precursors, which were electrodeposited at a) -1.3V and b) -1.6V, and $CuInS_2$ films which were formed via sulfurization of precursors electrodeposited at c) -1.3V and d) -1.6V.

Raman Spectroscopy Characterization

Raman spectroscopy is a crucial characterization technique to investigate the secondary phases forming at the surface, particularly CuS. The Raman spectra of films forming the $CuInS_2$ phase together with secondary phases are shown in **Fig. 6**, in the range 200-600 cm^{-1}.The films show clear peaks for $CuInS_2$ due to the presence of two distinct $CuInS_2$ phases [45,46]: the Raman peak for the chalcopyrite phase has been reported to be around

290-295cm^{-1} while the CuAu-type ordered phase have a Raman peak around 300-307cm^{-2} [46,47]. The precursor that was deposited at -1.3V with Cu/In ratio 1.22 shows the smallest amount of the secondary phase, in agreement with crystal structure data. A Cu-poor film (Cu/In= 0.86), and the most Cu-rich film (Cu/In=2.08) formed $CuInS_2$ phases, in parallel with CuS and In_2O_3 phases. The relative intensity of the peaks for $CuInS_2$ is lower for these two films in comparison to other Cu-rich films. Peaks from $CuIn_5S_8$ phase were not observed. The CuS peak around 474 cm^{-1} was present in all films, and the intensity ratio of the $CuInS_2$ peak vs. the CuS peak was the highest for uniform and compact films with Cu/In ratio 1.22. In_2O_3 (an n-type semiconductor with band gap ~2.7 to 3.75eV [48] was detected in some of the alloys; however, this phase has not been observed for any of the films in the XRD patterns, suggesting that this phase is close to or at the surface, and is probably generated by surface oxidation. Two more peaks are observed at 382 and 407 cm^{-1}, corresponding to MoS_2 [49]. This phase is forming during sulfurization at the interface between Mo substrates and the $CuInS_2$ films.

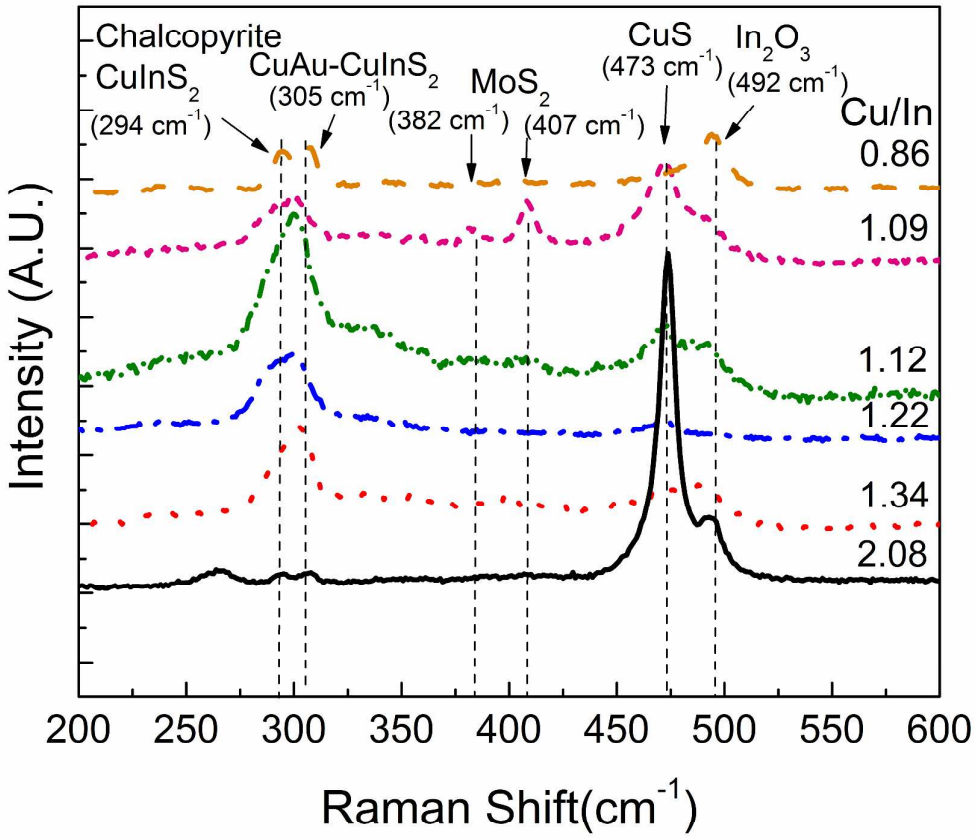

Fig. 6 Raman Spectrum of Cu-In precursors after sulfurization, precursors electrodeposited from sol. 3.

Photoelectrochemical Characterization

A weak photoelectrochemical response was detected with Cu-poor films (Cu/In ratio 0.86), and no photoelectrochemical current was observed for the most Cu-rich film with Cu/In ratio > 2. The photoelectrochemical current vs. potential data for $CuInS_2$ films with Cu/In ratio 1.09-1.34 is shown in **Fig. 7**; these films include $CuInS_2$ films with the chalcopyrite and the ordered CuAu-type structure. The potential was swept from -0.4V to -1.05V at 10mV/s to avoid electrochemical Eu^{3+} reduction. The cathodic photoelectrochemical current response began to arise around -0.5V, indicating that the $CuInS_2$ films are p-type. The dark current measurement on Mo substrate is shown in the inset of **Fig. 7** with a continuous line.

The photoelectrochemical current did not saturate within the selected potential range; the fast current transients, in addition, suggest a limited density of recombination states. The largest photoelectrochemical response, 0.15mA/cm^2, was obtained at -0.95 V with a smooth film electrodeposited at -1.3V, Cu/In ratio 1.22. The lowest photoelectrochemical current response, 0.05mA/cm^2, was observed with a dendritic film that was electrodeposited at -1.6V, Cu/In ratio 1.12. Photoelectrochemical characterization in $Eu(NO_3)_3$ solution for p-type $CuInS_2$ films, has been reported by others to result in a photoelectrochemical response around 0.1-1.5mA/cm^2 [50,51].-Ikeda et al. in particular investigated both the photoelectrochemical current and the solar cell efficiency of $CuInS_2$ films obtained by spray pyrolysis. Photoelectrochemical response of their $CuInS_2$ film was around ~1.5mA/cm^2 in an aqueous $Eu(NO_3)_3$ solution under chopped illumination from a 300 W Xenon lamp and the efficiency of this solar cell was 5.1% [52]. Unfortunately, no actual incident power at the target sample was reported in this work, making it impossible to compare these data with our data.

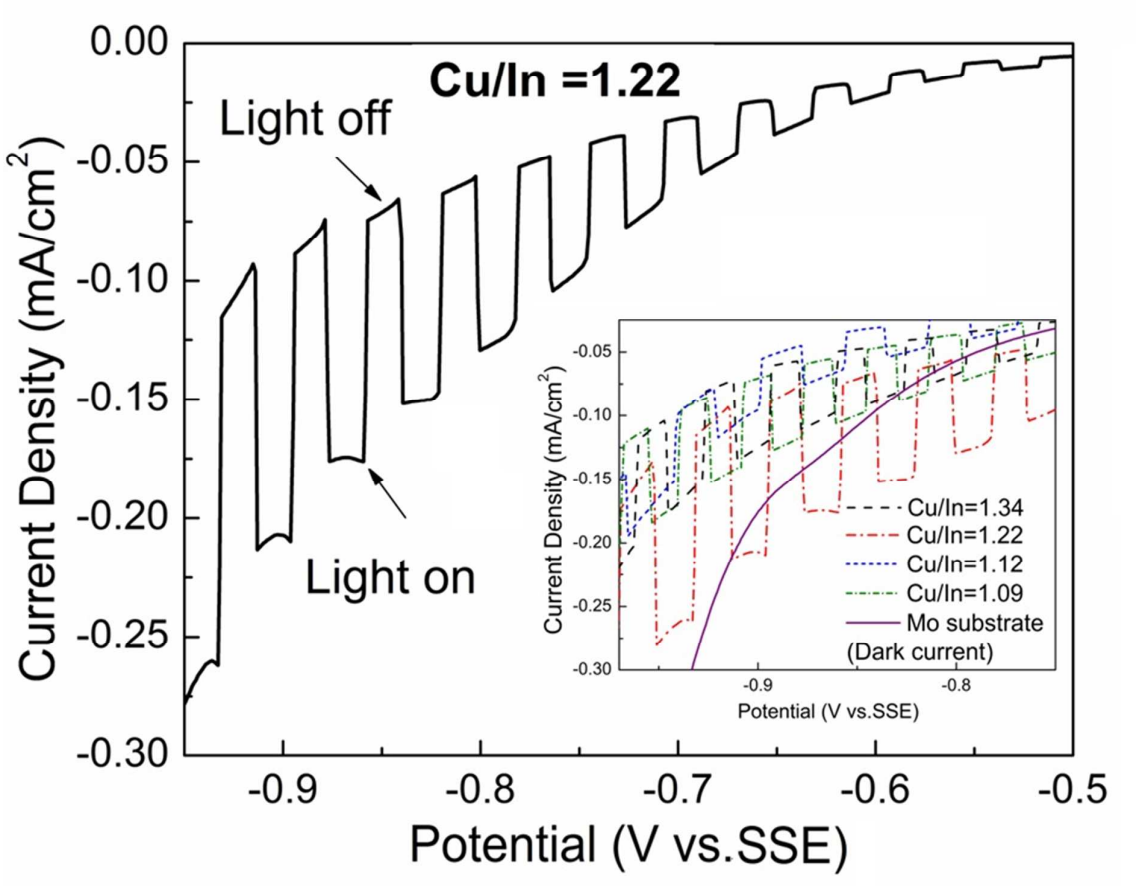

Fig. 7 Photoelectrochemical behavior of $CuInS_2$ film with Cu/In ratio 1.22 and photoelectrochemical responses of Cu-In precursors after sulfurization, precursors electrodeposited from sol. 3 (inset).

No definite correlation between photoelectrochemical response and composition has been found in our study, but overall the photoelectrochemical response was stronger for precursors that were electrodeposited at more positive potentials. This suggests that photoelectrochemical response behavior is not only dependent on the purity of the $CuInS_2$ phase and the precursor composition but also – in this case mainly – on the deposition potential, which has a critical influence on the morphology of the precursor, particularly at high applied overpotentials.

Mott-Schottky (M-S) plots for $CuInS_2$ films are shown in **Fig. 8**. The negative slope values of the linear fit indicate that all the $CuInS_2$ films are p-type, supporting the photocurrent data. **Table 1** shows the flat band potential V_{FB}, carrier concentration and photoresponse behavior for $CuInS_2$ films. The carrier density increased, and the V_{FB} shifted to more negative values with increasing Cu/In ratio, similar to reports for p-type $CuInS_2$ films formed by sulfurizing Cu-In precursors containing $Cu_{11}In_9$ intermetallic compound [52]. An increase in carrier density has also been observed in Cu-rich films for both $CuInS_2$ and $CuInSe_2$ [52,53]. A very high doping density, between $6.65x10^{20}$ and $2.86x10^{21}$ cm^{-3}, and flat band potentials between -0.005 and -0.145 V were extracted from the M-S plots. The room temperature carrier concentration is usually above 10^{16} cm^{-3} for Cu-rich $CuInS_2$ films and carrier densities up to 10^{20} cm^{-3} have been reported in the literature based on both computational and experimental results [52, 54-57]. The wide range of carrier densities being observed in the present work can be in part attributed to the high Cu fraction, but sulfurization and cooling conditions may have an important effect on these characteristics as well [56, 58]. The carrier densities observed in our study are 1-5 orders of magnitude higher than those reported by others. This may be due to the slow cooling conditions utilized in this work with respect to the constant cooling rate used in Ref. [56] and to the remaining CuS phases in the films.

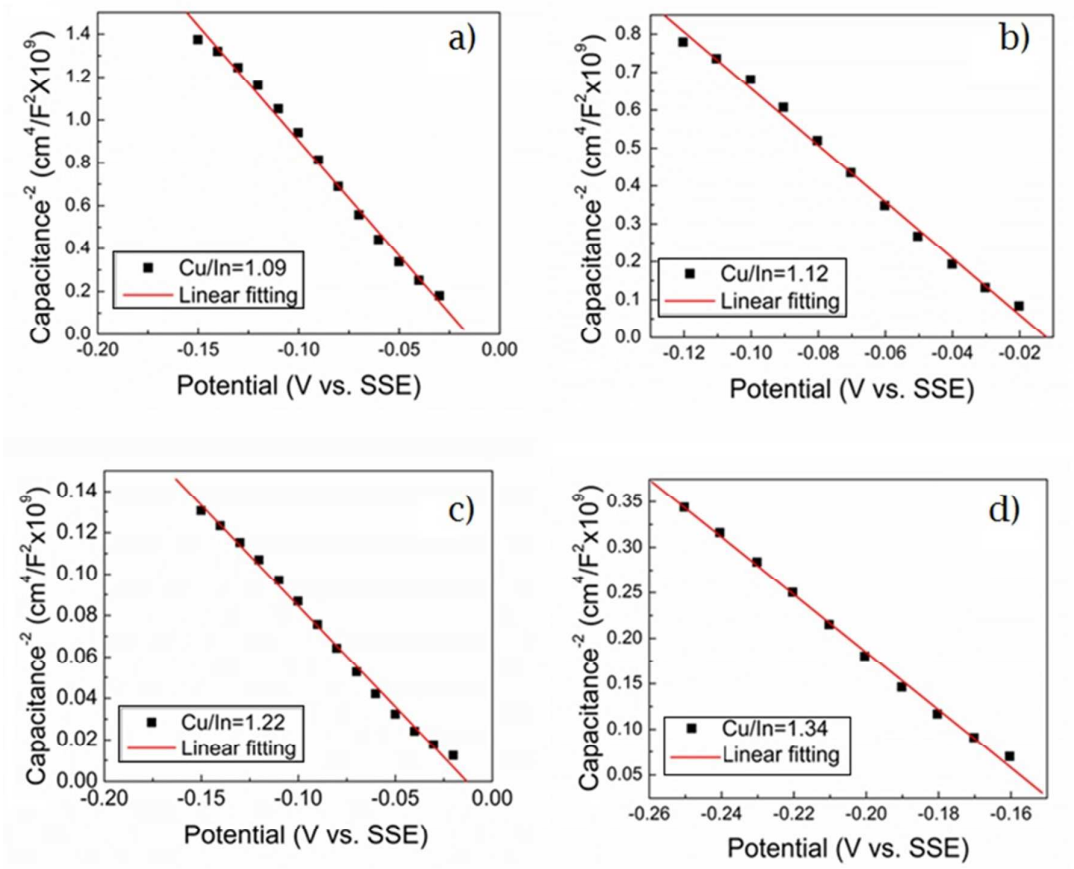

Fig. 8 Mott-Schottky plots (f=10 kHz) at pH value of 5.7,for $CuInS_2$ films with Cu/In ratio a) 1.09, b)1.12, c)1.22 and d)1.34.

Conclusion

Electrodeposition of Cu-In was investigated, focusing on the formation of close to equiatomic compositions; selected alloys were sulfurized to form $CuInS_2$ absorber layers. In-rich precursors with Cu/In ratio between 0.07 and 0.21 showed a low fraction of intermetallic compounds, resulting in the predominant formation of an In-rich phase. Alloys within the Cu/In composition ratio between 0.97 and 1.17 exhibited large fractions of intermetallic phases and upon sulfurization formed p-type $CuInS_2$ with CuS as a secondary phase. The p-type $CuInS_2$ chalcopyrite phase coexists with the CuAu-type ordered $CuInS_2$ phase.

The composition and morphology of the alloy precursors have a strong influence on the quality of the absorber films. Cu-rich precursors close to the stoichiometric value were

electrodeposited at relatively positive potentials, resulting in compact and fine grains that upon sulfurization formed dense $CuInS_2$ films with a small amount of secondary phases. In contrast, precursors electrodeposited at high overvoltages formed rough dendrites and larger amounts of secondary phases. A maximum photoelectrochemical response of 0.15 mA/cm^2 was observed from alloy precursors with a Cu/In ratio 1.22, exhibiting a compact morphology.

Acknowledgement

This work was financially supported in part by the NSF grant CMMI #1131571. BU was funded by the Republic of Turkey Ministry of National Education.

References

[1] Renewables 2013 Global Status Report, 2013. doi:ISBN 978-3-9815934-0-2.

[2] M.A. Green, , Prog. Photovoltaics Res. Appl., 2009, 17,183–189. doi:10.1002/pip.892.

[3] D.E. Carlson, C.R. Wronski, Appl. Phys. Lett., 1976, 28, (1976) 671–673. doi:10.1063/1.88617.

[4] I. Visoly-Fisher, S.R. Cohen, A. Ruzin, D. Cahen, , Adv. Mater. 16 (2004) 879–883. doi:10.1002/adma.200306624.

[5] I. Repins, M.A. Contreras, B. Egaas, C. Dehart, J. Scharf, C.L. Perkins, , Prog. Photovolt Res. App. ,2008, 235–239. doi:10.1002/pip.

[6] H. Yan, Z. Zhou, H. Lu, Photovoltaic industry and market investigation, in: 1st Int. Conf. Sustain.PowerGener.Supply,SUPERGEN'09,2009, doi:10.1109/SUPERGEN.2009.5348104.

[7] S. Siebentritt, M. Igalson, C. Persson, S. Lany, ,,201, 390–410. doi:10.1002/pip.936.

[8] A. A. Rockett, , Curr. Opin. Solid State Mater. Sci. 14,2010, 143–148. doi:10.1016/j.cossms.2010.08.001

[9] K.-W. Cheng, W.-H. Chiang, J. Electroanal. Chem., 2011,661,57–65. doi:10.1016/j.jelechem.2011.07.013.

[10] J.J. Loferski, J. Appl. Phys., 1956,27 ,777–784. doi:10.1063/1.1722483.

[11] X. Shang, Z. Wang, M. Li, L. Zhang, J. Fang, J. Tai,Y He, Thin Solid Films, 2014,550,649–653. doi:10.1016/j.tsf.2013.10.047.

[12] C. Broussillou, M. Andrieux, M. Herbst-Ghysel, M. Jeandin, J.S. Jaime-Ferrer, S. Bodnar, E. Morin, Sol. Energy Mater. Sol. Cells,2011, 95 ,S13–S17. doi:10.1016/j.solmat.2011.01.037.

[13] J. Klaer, J. Bruns, R. Henninger, K. Siemer, R. Klenk, K. Ellmer, D. Braunig, Semicond. Sci. Technol. 13 (1999) 1456–1458. doi:10.1088/0268-1242/13/12/022.

[14] J. Eberhardt, K. Schulz, H. Metzner, J. Cieslak, T. Hahn, U. Reislöhner, W. Witthuhn, Epitaxial and polycrystalline $CuInS_2$ thin films: A comparison of opto-electronic properties, Thin Solid Films. 515 (2007) 6147–6150. doi:10.1016/j.tsf.2006.12.039.

[15] X.-P. Liu, L.-X. Shao, , Surf. Coatings Technol., 2007201,5340–5343. doi:10.1016/j.surfcoat.2006.07.182.

[16] J.D. Harris, K.K. Banger, D. A. Scheiman, M. A. Smith, M.H.C. Jin, A.F. Hepp, , Mater. Sci. Eng. B Solid-State Mater. Adv. Technol., 2003, 98 ,150–155. doi:10.1016/S0921-5107(03)00041-2.

[17] F. Cui, L. Wang, Z. Xi, Y. Sun, D. Yang, J. Mater. Sci. Mater. Electron, 2009, 20, 609–613. doi:10.1007/s10854-008-9773-3.

[18] D. Lee, J. Kim, Sol. Energy Mater. Sol. Cells. 2011, 95,245–249. doi:10.1016/j.solmat.2010.04.066.

[19] Y. Bourlier, R. Bernard, C. Lethien, P. Roussel, M. Zegaoui, M. Bouazaoui, N. Rolland, P.A. Rolland, , Appl. Phys. Express., 2012, 5. doi:10.1143/APEX.5.125801.

[20] X. Xu, F. Wang, J. Liu, J. Ji, Electrochim. Acta., 2010, 55 4428–4435. doi:10.1016/j.electacta.2010.02.077.

[21] S.M. Lee, S. Ikeda, Y. Otsuka, W. Septina, T. Harada, M. Matsumura, Electrochim. Acta., 2012, 79, 189–196. doi:10.1016/j.electacta.2012.06.103.

[22] J. Yuan, C. Shao, L. Zheng, M. Fan, H. Lu, C. Hao, D. Tao, Vacuum., 2014, 99, 196–203. doi:10.1016/j.vacuum.2013.06.005.

[23] G. Zangari, *ECS Interface*, 2011, Summer Edition, 31-32.

[24] X.H. Xu, F. Wang, J.J. Liu, K.C. Park, M. Fujishige, , Sol. Energy Mater. Sol. Cells., ,2011, 95 ,791–796. doi:10.1016/j.solmat.2010.10.025.

[25] S.M. Lee, S. Ikeda, Y.O. Harada, M. Matsumura, , J. Non. Cryst. Solids., 2012, 358,2424–2427. doi:10.1016/j.jnoncrysol.2011.12.043.

[26] A. Joswig, M. Gossla, H. Metzner, U. Reislöhner, T. Hahn, W. Witthuhn, , Thin Solid Films.,2007, 515, 5921–5924. doi:10.1016/j.tsf.2006.12.053.

[27] D. Liang, B. Unveroglu. G. Zangari, J. Elec. Soc., 2014, 161613–619. doi: 10.1149/2.1191410jes.

[28] C. Kind, C. Feldmann, A. Quintilla, E. Ahlswede, , Chem. Mater., 2011,23, 5269-5274. doi:10.1021/cm2024668.

[29] V. Deprédurand, D. Tanaka, Y. Aida, M. Carlberg, N. Fèvre, S. Siebentritt, , J. Appl. Phys., 2014, 115 , 044503. doi:10.1063/1.4862181.

[30] M. Alt, H.J. Lewerenz, R. Scheer, , J. Appl. Phys. 81, 1997, 956. doi:10.1063/1.364224.

[31] T. Walter, R. Menner, Ch. Koble and H. W. Schock, Proc. 12th European Photovoltaic Solar Energy Conf., Amsterdam, H. S. Stephens & Associates, Oxfordshire , 1994, p. 1755

[32] R. Scheer, T. Walter, H.W. Schock, M.L. Fearheiley, H.J. Lewerenz, Appl. Phys. Lett., 1993, 63,3294. doi:10.1063/1.110786.

[33] T. Watanabe, H. Nakazawa, M. Matsui, Japanese J. Appl. Physics, 1998, Part 2 Lett. 37. doi:10.1143/JJAP.37.L1370.

[34] T.T. John, M. Mathew, C.S. Kartha, K.P. Vijayakumar, T. Abe, Y. Kashiwaba, , Sol. Energy Mater. Sol. Cells., 2005, 89 , 27–36. doi:10.1016/j.solmat.2004.12.005.

[35] J. Álvarez-García, A. Pérez-Rodríguez, A. Romano-Rodríguez, J.R. Morante, L. Calvo-Barrio, R. Scheer, R. Klenk, J. Vac. Sci. Technol. A Vacuum, Surfaces, Film., 2001,19 ,232. doi:10.1116/1.1329123.

[36] S.-H. Wei, S. Zhang, A. Zunger, , Phys. Rev. B., 1999, 59,R2478–R2481. doi:10.1103/PhysRevB.59.R2478.

[37] M. Gusain, P. Kumar, R. Nagarajan, RSC Adv., 2013, 3,) 18863. doi:10.1039/c3ra41698d.

[38] D.Y. Lee, J. Kim, , Thin Solid Films., 2010, 518,6537–6541. doi:10.1016/j.tsf.2010.03.062.

[39] J. Alvarez-García, A. Pérez-Rodríguez, B. Barcones, A. Romano-Rodríguez, J.R. Morante, A. Janotti,S. Wei, R. Scherr, , Appl. Phys. Lett., 2002, 80,562–564. doi:10.1063/1.1435800.

[40] R. Memming, , J. Electrochem. Soc., 1978, 125,117. doi:10.1149/1.2131374.

[41] D. Lincot, H.Gomez Meier, J. Kessler, J. Vedel, Sol. Energy Mater., 1990, 20 67–79.

[42] J. Qiu, Z. Jin, J. Qian, Y. Shi, W. Wu, , J. Cryst. Growth., 2005, 282, 421–428. doi:10.1016/j.jcrysgro.2005.05.049.

[43] C. von Klopmann, J. Djordjevic, E. Rudigier, R. Scheer, J. Cryst. Growth., 2006,289, 121–133. doi:10.1016/j.jcrysgro.2005.10.106.

[44] K.I. Popov, S.S. Djovik, B.N. Grgur, New York 2002, and references therein.

[45] D.Y. Lee, J. Kim, Sol. Energy Mater. Sol. Cells.,2011, 95,245–249. doi:10.1016/j.solmat.2010.04.066.

[46] E. Rudigier, B. Barcones, I. Luck, T. Jawhari-Colin, A. Pérez-Rodríguez, R. Scheer, J. Appl. Phys., 2004, 95, 5153–5158. doi:10.1063/1.1667009.

[47] I. Oja, M. Nanu, A. Katerski, M. Krunks, A. Mere, J. Raudoja, A. Goossens, Thin Solid Films,2005, 480-481,82–86. doi:10.1016/j.tsf.2004.11.013.

[48] Aron Walsh, Juarez L. F. Da Silva, Su-Huai Wei, C. Körber, A. Klein, L. F. J. Piper, Alex DeMasi, Kevin E. Smith, G. Panaccione, P. Torelli, D. J. Payne, A. Bourlange, and R. G. Egdell, Phys. Rev. Lett.,2008, **100**, 167402.

[49] H. Li, Q. Zhang, C.C.R. Yap, B.K. Tay, T.H.T. Edwin, A. Olivier, D. Baillargeat, , Adv. Funct. Mater., 2012, 22 , –1390. doi:10.1002/adfm.201102111.

[50] P.J. Dale, A.P. Samantilleke, G. Zoppi, I. Forbes, S. Roncallo, L.M. Peter, , E.C.S. Transactions, T.E. Society, 2007, 6, 2007 535–546. doi:10.1149/1.2731222.

[51] S. Ikeda, M. Nonogaki , W. Septina, G. Gunawan, T. Harada, M. Matsumura, , Catal Sci Technol, 2013, 3, 1849. doi: 10.1039/c3cy00020f.

[52] K-W. Cheng, Y-C. Wu,Y-T. Hu, Mater Res Bull, 2013, 48, 2457–2468. doi: 10.1016/j.materresbull.2013.02.085.

[53] S. Siebentritt, L. Gütay, D. Regesch, Y. Aida, V. Depredurand , Sol Energy Mater Sol Cells, 2013, 119, 18–25. doi: 10.1016/j.solmat.2013.04.014.

[54] A. M. Martinez , L. G. Arriaga,A. M. Fernández,U. Cano , Mater Chem Phys, 2004, 88, 417–420. doi: 10.1016/j.matchemphys.2004.08.009.

[55] B. Tell, J. L. Shay, H. M. Kasper, J Appl Phys, 1972, 43, 2469–2470. doi: 10.1063/1.1661532 1972.

[56] M. Krunks M, A. Mere, A. Katerski, V. Mikli, J. Krustok, Thin Solid Films, 2006, 511-512, 434–438. doi: 10.1016/j.tsf.2005.11.072.

[57] S. R. Kodigala, Thin Films and Nanostructures: $Cu(In_{1-x}Ga_x)Se_2$ based thin film solarcells, Elsevier Science, 2011, 35, p. 368.

[58] K. Yoshino, K. Nomoto,A. Kinoshita, T. Ikari, Y. Akaki, T. Yoshitake, J Mater Sci Mater Electron, 2008, 19, 301–304. doi: 10.1007/s10854-007-9334-1.